

# Optimizing the indirect search for dark matter with the CTA

J. Mamprim & V. de Souza

<sup>1</sup> Instituto de Física de São Carlos, Universidade de São Paulo  
email:juliagouveamamprim@usp.br, vitor@ifsc.usp.br

**Abstract.** This work proposes to investigate the potential of the Cherenkov Telescope Array (CTA) for the indirect detection of DM through a gamma-ray signal produced by the annihilation of dark matter particles at the Galactic Center region. We calculated the  $J$ -factor map and gamma-ray flux for three different annihilation channels, considering a point-source, and compared the results with the CTA flux sensitivity, concluding that the observatory would be able to provide a  $5\sigma$  detection of the flux.

**Resumo.** Neste trabalho, propomos investigar o potencial do Cherenkov Telescope Array (CTA) para a detecção indireta de Matéria Escura (DM) através de um sinal de raios gama produzido pela aniquilação de partículas de matéria escura na região do Centro Galáctico. Calculamos o mapa de  $J$ -factor e o fluxo de raios gama para três canais de aniquilação diferentes, considerando uma fonte pontual, e comparamos os resultados com a sensibilidade de fluxo do CTA, concluindo que o observatório seria capaz de fornecer uma detecção de  $5\sigma$  do fluxo em questão.

**Keywords.** Galaxy: center – dark matter – gamma rays: general

## 1. Introduction

The most promising theories regarding the dark matter (DM) paradigm address it as a particle that falls outside of the Standard Model, thermally produced at the early Universe. It is a neutral, stable, and non-baryonic elementary particle that constitutes approximately 85% of the Universe's total matter. In high density environments of the Universe, DM may self-annihilate producing a strong gamma-ray signal that, depending on its properties, could be detected by current and future experiments.

### 1.1. Dark matter evidences

The evidences for the existence of DM are diverse and manifest on various scales. We briefly list the most significant evidences below.

1. **Galaxy Cluster Dynamics.** The motion of galaxies within galaxy clusters suggests the presence of significant mass that is not visible. This fact was first observed by Fritz Zwicky in 1933, when he used the Virial Theorem to infer the velocity of the galaxies in the Coma cluster Zwicky (1933).
2. **Galactic Rotation Curves.** Observations of galactic rotation velocities indicate that galaxies rotate much faster than what is expected based on the visible mass alone. The presence of this missing mass, likely in the form of dark matter, is inferred to account for this anomaly Rubin (1970).
3. **Cosmic Microwave Background (CMB) Anisotropies.** The CMB anisotropies exhibit frequency components in their distribution, which can be described through a power spectrum featuring a series of peaks and valleys. The peaks provide details about the density of ordinary matter, and can be explained more accurately by considering the presence of dark matter in the early Universe Kolb (2018).
4. **The Bullet Cluster.** In the collision between two galaxy clusters, the normal matter and dark matter components were found to behave differently. Observations revealed that the hot X-ray-emitting gas, representing the majority of normal matter, was displaced during the collision. However, the gravitational lensing effect, caused by the bending of light

due to gravity, showed the presence of unseen mass (dark matter) at the location of the lensing, separate from the X-ray-emitting gas. This separation between the distributions of normal and dark matter in the Bullet Cluster strongly supports the idea that dark matter is a distinct, non-interacting component of the universe, providing compelling evidence for its existence Profumo (2017).

5. **Large-Scale Structure Formation.** The distribution of galaxies and other structures on large scales is influenced by the gravitational potential of dark matter since its formation. Cosmological simulations that include the dark matter component provide a better match to observed structures Mo (2010).

These lines of evidence collectively support the existence of dark matter. Still, its nature remains one of the fundamental mysteries in modern astrophysics and particle physics.

### 1.2. WIMP dark matter

Weakly interacting massive particles (WIMPs) are very popular candidates for dark matter. Its attractiveness comes mainly from the fact that a thermal relic with weak scale mass and annihilation cross-section into Standard Model (SM) naturally yields an roughly correct cosmological relic abundance Fortes (2023).

The WIMPs self-annihilation process could occur in regions of high dark matter density, such as the center of galaxies or galaxy clusters, potentially generating a flux of SM particles, including gamma rays. The detection of the photon fluxes that come from DM self-annihilations or decays is called indirect detection, and constitutes one of the main goals of high energy gamma-ray observatories.

### 1.3. Cherenkov Telescope Array

Ground-based gamma-ray astronomy is a burgeoning field with significant scientific potential. The current major arrays of IACTs (Imaging Atmospheric Cherenkov Telescope), including H.E.S.S., MAGIC, and VERITAS, have showcased the immense physics potential at energies around TeV, demonstrating the

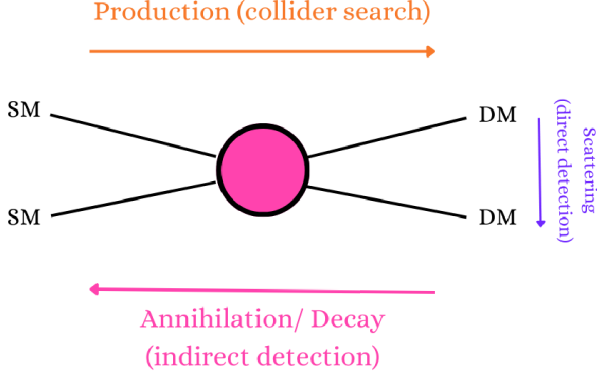


**FIGURE 1.** Representation of the processes of production, scattering and annihilation/decay of DM particles.

maturity of the detection technique. The upcoming Cherenkov Telescope Array (CTA) is expected to revolutionize our understanding of the high-energy universe, addressing fundamental questions in physics.

CTA will have arrays of IACTs on two sites (one in Paranal, Chile, and the other at La Palma, Canary Islands, Spain), granting access to the entire sky, once the sites will be positioned in two hemispheres. With three different sizes of telescopes (Large-Sized Telescope (LST), Medium-Sized telescope (MST) and Small-Sized Telescope (SST)), the CTA observatory aims to enhance the sensitivity level of current instruments by a factor of ten at 1 TeV. It will have a substantially increased detection area, what elevates the photon rate, enabling observation of phenomena on the shortest timescales, improving angular resolution and expanding the field of view.

A key aspect of the CTA program involves the search for WIMP dark matter annihilation signatures, considering the expected cross-section for a thermal relic across a broad spectrum of masses. This feature renders CTA highly complementary to alternative approaches, including high-energy particle collider and direct-detection experiments.

In this work, we will consider the CTA "Alpha configuration" for the southern and northern arrays of the observatory. It consists of 4 Large-Sized Telescopes and 9 Medium-Sized Telescopes at the Northern array, with a coverage area of  $\sim 0.25\text{km}^2$ , and 14 Medium-Sized Telescopes and 37 Small-Sized Telescopes at the Southern array, with a coverage area of  $\sim 3\text{km}^2$  CTA Consortium (2018).

## 2. Methods

Indirect dark matter searches involve detecting an excess of standard model particles resulting from DM annihilation or decay. This approach presents numerous potential targets (such as the Galactic Center and Dwarf Spheroidal Galaxies) and enables us to explore energy levels that are beyond the reach of Earth-based experiments.

Regarding the CTA science, we will analyse the flux of gamma rays coming from a specific target: the Galactic Center. For a DM particle that is its own antiparticle, the differential flux of photons from the annihilation process is given by

$$\frac{d\Phi_\gamma}{dE_\gamma}(E_\gamma, \Delta\Omega) = \frac{\langle\sigma v\rangle}{8\pi m_{\text{DM}}^2} \frac{dN}{dE_\gamma} \times J(\Delta\Omega). \quad (1)$$

The first term corresponds to particle physics information, relating the nature of DM properties and their interactions.  $\langle\sigma v\rangle$

is the thermal-averaged velocity-weighted cross-section,  $m_{\text{DM}}$  is the dark matter particle's mass, and  $dN/dE_\gamma$  is the annihilation differential spectrum into gamma rays. The second term, named J-factor, is astrophysical and contains information on how DM is spatially distributed around the galaxy and in which direction the observation is being made. More explicitly, the J-factor can be written as

$$J(\Delta\Omega) = \int d\Omega \int_{\text{l.o.s.}} ds \rho_{\text{DM}}^2(r(s, \theta)), \quad (2)$$

where  $\rho_{\text{DM}}$  is the dark matter density profile, and the integral is made along a line of sight (l.o.s) over a solid angle  $\Delta\Omega$ . It is convenient to parametrize the density function as a function of  $r$ , between the observer and the target, with  $r$  becoming

$$r = \sqrt{s^2 + r_\odot^2 - 2sr_\odot \cos\theta}, \quad (3)$$

where  $s$  is the distance along the l.o.s,  $\theta$  is the angle between the observation direction and the GC, and  $r_\odot$  is the distance of the Sun to the GC. We assume  $r_\odot = 8.5\text{kpc}$ .

It is important to emphasize that the J-factor strongly depends on the chosen halo density profile, specially for regions of small radii. We took the Einasto profile, described by

$$\rho_{\text{Einasto}} = \rho_s \exp\left(-\frac{2}{\alpha} \left[\left(\frac{r}{r_s}\right)^\alpha - 1\right]\right), \quad (4)$$

with  $r_s$  and  $\rho_s$  being the radius and density at which the logarithmic slope of the density is  $-2$ , respectively. The parameter  $\alpha$  controls the curvature of the profile. As in Ref. Fortes (2023), we set  $r_s = 20\text{kpc}$  and  $\alpha = 0.17$ .  $\rho_s$  was calculated assuming that the local density is  $\rho_{\text{DM}}(r_\odot) = 0.39\text{ GeV}/\text{cm}^3$ .

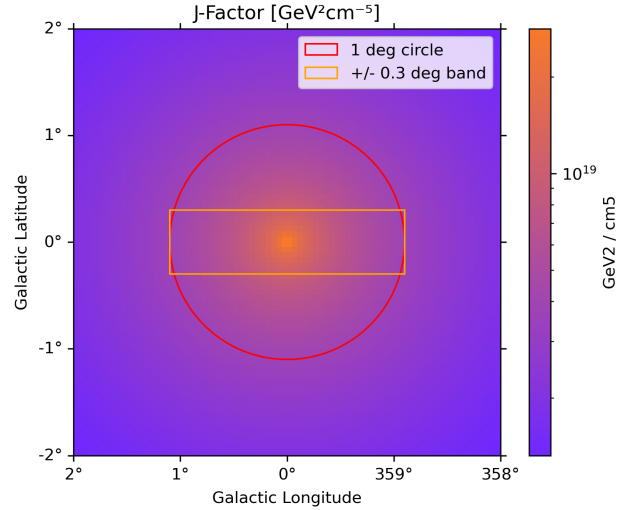


**FIGURE 2.** J-factor map around the GC region. The orange contour is the  $\pm 0.3^\circ$  exclusion band, while the red contour indicates a  $1^\circ$  circular region. Generated with Gammapy Donath (2023).

The J-factor map is shown in Figure 2. It was subdivided in squared spatial bins of size  $0.05^\circ$ , which is consistent with the CTA's angular resolution of  $0.05^\circ$  or less for energies above 1 TeV CTA Consortium (2018). To minimize the numerous background gamma-ray sources located at the Galactic Center region, a  $\pm 0.3^\circ$  band in Galactic latitude was excluded. The integrated J-factor in a circular region of  $1^\circ$  centered at the GC, excluding

the  $\pm 0.3^\circ$  band, gives the value  $J = 4.38 \times 10^{21} \text{GeV}^2/\text{cm}^5$  for the assumed density profile.

The gamma-ray spectrum per annihilation for many different channels is computed in Cirelli (2011). Figure 3 shows the spectrum for the channels  $\tau\tau$ ,  $b\bar{b}$  and  $W^+W^-$ , considering  $m_{\text{DM}} = 1 \text{TeV}$  and  $m_{\text{DM}} = 10 \text{TeV}$ , and considering the thermal-relic annihilation cross-section, i.e.,  $\langle\sigma v\rangle = 3 \times 10^{-26} \text{GeV}^2/\text{cm}$ .

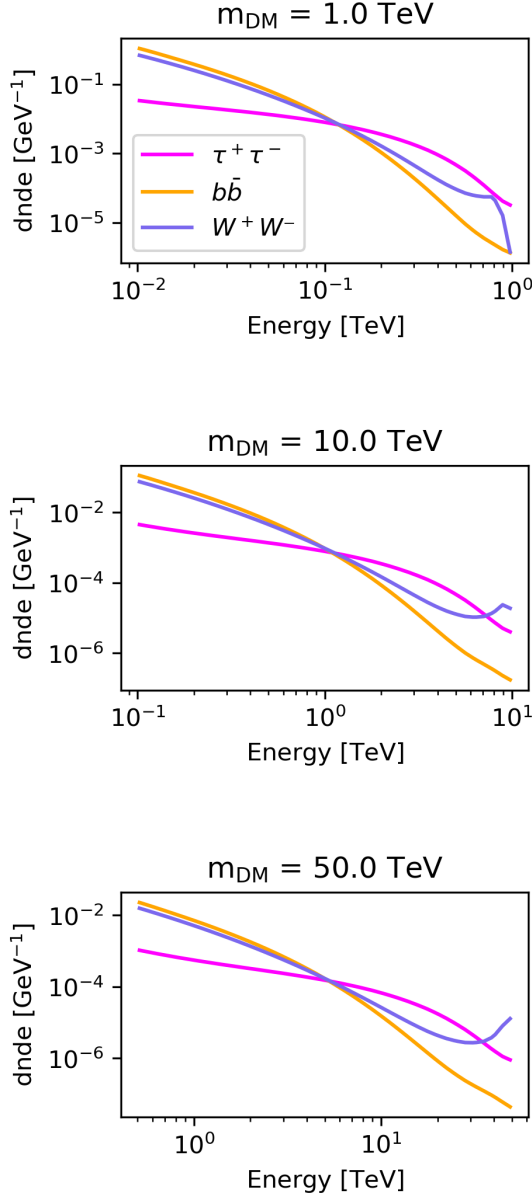


**FIGURE 3.** The gamma-ray spectrum per annihilation.

In order to compare the expected gamma-ray flux from DM annihilation at the GC with the CTA's future detection capability, it is also important to determine the flux sensitivity of the CTA, calculating the number of observable events, which requires setting an Instrument Response Function (IRF), the live time of observation  $T_{\text{obs}}$  and the detector's effective area  $A_{\text{eff}}$ . Then, the number of photon counts is given by

$$N_{\text{DM}} = \frac{T_{\text{obs}} J \langle\sigma v\rangle}{8\pi m_{\text{DM}}^2} \int_{E_{\text{min}}}^{E_{\text{max}}} \frac{dN_{\text{DM}}}{dE}(E) A_{\text{eff}}(E) dE. \quad (5)$$

Figure 4 shows the CTA's differential flux sensitivity compared to other gamma-ray observatories. It's calculated for a point-like source that exhibits a power-law spectra

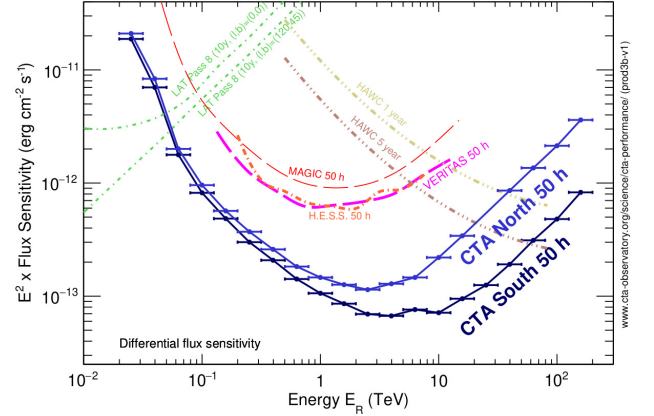


**FIGURE 4.** Differential energy flux sensitivities for CTA (south and north), compared to other gamma-ray instruments CTA Consortium (2018).

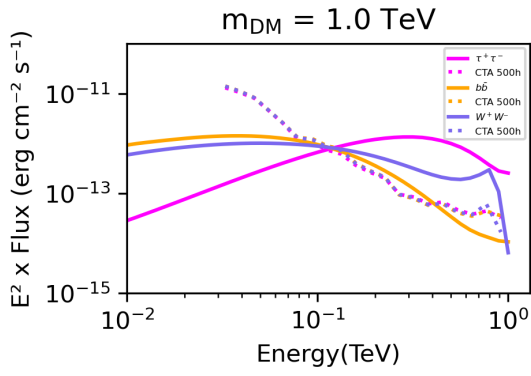
### 3. Results

The gamma-ray flux from a point-like source was calculated as in eq. (1), for the annihilation channels displayed in Figure 3 and considering the integrated J-factor in a circular region of  $1^\circ$  centered at the GC, excluding the  $\pm 0.3^\circ$  band ( $J = 4.38 \times 10^{21} \text{GeV}^2/\text{cm}^5$ ), for the Einasto density profile. The results for the flux times energy squared are shown in Figure 4 (continuous lines).

The differential sensitivity curves (dashed lines) are defined as the minimum flux needed by CTA to obtain a 5-standard-deviation detection of a point-like source, calculated in non-overlapping logarithmic energy bins (five per decade) CTA Consortium (2018). Following the CTA consortium methodology, we require at least ten detected gamma rays per energy bin, and a signal/background ratio of at least 1/20. The instrument response functions (IRFs) we used can be downloaded on CTA's website, and illustrate the preliminary performance of the observatory during its initial construction phase with the approved "Alpha Configuration," derived from detailed Monte Carlo (MC) simulations of the consortium. The observation time is set to 500h, assuming a source at the GC with a  $1^\circ$  radius.

### 4. Conclusions

We calculated the gamma-ray flux from DM annihilating at the Galactic Center, considering the Einasto density profile and for three different annihilation channels and masses. Later, we compared these results to the flux sensitivity curves derived from CTA's preliminary IRFs for the "Alpha Configuration", for a point-like source. As Figure 5 shows, CTA would be able to detect a gamma-ray signal in the case under analysis. However, since dark matter sources are in fact extended, and not point-like, a more strict approach is to calculate the flux and sensitivity for every bin of the J-factor map, and not for the integrated region, and that is what we will do in the future. Then, it will be possible to set an upper limit on the dark matter particle's annihilation cross-section for different models, which is the main goal of this project.



Profumo, S. 2017, An introduction to particle dark matter. World Scientific Publishing Company  
 Rubin, V. C., Ford, J. R., & Kent, W. 1970, ApJ, 159, 379  
 Zwicky, F. 1933, Helvetica Physica Acta, 6, 110

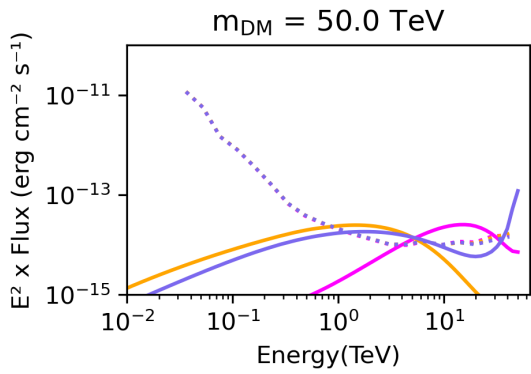
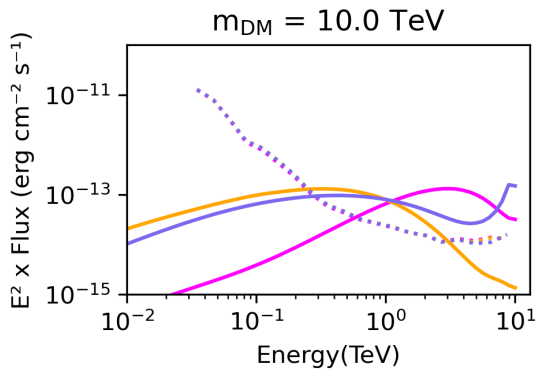


**FIGURE 5.** Differential energy flux for three annihilation channels, compared to the CTA’s 500h differential flux sensitivities.

*Acknowledgements.* J.M. and V.d.S. acknowledge FAPESP Projects 2022/16842-0 and 2021/01089-1. The authors acknowledge the National Laboratory for Scientific Computing (LNCC/MCTI, Brazil) for providing the HPC resources of the SDumont supercomputer (<http://sdumont.lncc.br>). V.d.S. acknowledges CNPq.

## References

Cirelli, M. et al. 2011, JCAP, 3, 51  
 CTA Consortium et al. 2018, Science with the Cherenkov Telescope Array, World Scientific  
 Donath, A. et al. 2023, arXiv:2308.13584  
 Fortes, G. N. et al. 2023, JCAP, 7, 43  
 Kolb, E. 2018, The early universe, CRC press  
 Mo, H., van den Bosch, F., & White, S. 2010, Galaxy formation and evolution, Cambridge University Press